

Asymptotic Limits and Zeros of Chromatic Polynomials and Ground State Entropy of Potts Antiferromagnets

Robert Shrock* and Shan-Ho Tsai**

Institute for Theoretical Physics
State University of New York
Stony Brook, N. Y. 11794-3840

Abstract

We study the asymptotic limiting function $W(\{G\}, q) = \lim_{n \rightarrow \infty} P(G, q)^{1/n}$, where $P(G, q)$ is the chromatic polynomial for a graph G with n vertices. We first discuss a subtlety in the definition of $W(\{G\}, q)$ resulting from the fact that at certain special points q_s , the following limits do not commute: $\lim_{n \rightarrow \infty} \lim_{q \rightarrow q_s} P(G, q)^{1/n} \neq \lim_{q \rightarrow q_s} \lim_{n \rightarrow \infty} P(G, q)^{1/n}$. We then present exact calculations of $W(\{G\}, q)$ and determine the corresponding analytic structure in the complex q plane for a number of families of graphs $\{G\}$, including circuits, wheels, biwheels, bipyramids, and (cyclic and twisted) ladders. We study the zeros of the corresponding chromatic polynomials and prove a theorem that for certain families of graphs, all but a finite number of the zeros lie exactly on a unit circle, whose position depends on the family. Using the connection of $P(G, q)$ with the zero-temperature Potts antiferromagnet, we derive a theorem concerning the maximal finite real point of non-analyticity in $W(\{G\}, q)$, denoted q_c and apply this theorem to deduce that $q_c(sq) = 3$ and $q_c(hc) = (3 + \sqrt{5})/2$ for the square and honeycomb lattices. Finally, numerical calculations of $W(hc, q)$ and $W(sq, q)$ are presented and compared with series expansions and bounds.

*email: shrock@insti.physics.sunysb.edu

**email: tsai@insti.physics.sunysb.edu

1 Introduction

An important question in graph theory is the following: using q different colors, what is the number of ways $P(G, q)$ in which one can color a graph G , having n vertices, such that no two adjacent vertices have the same color? The function $P(G, q)$, first introduced by Birkhoff [1], is a polynomial in q of order n and has been the subject of mathematical study for many years [2]-[3]; a recent review is Ref. [4]. Clearly, a general upper bound on a chromatic polynomial is $P(G, q) \leq q^n$, since the right-hand side is the number of ways that one can color the n -vertex graph G without any constraint. Consequently, it is of interest to study the limiting function

$$W(\{G\}, q) = \lim_{n \rightarrow \infty} P(G, q)^{1/n} \quad (1.1)$$

where the symbol $\{G\}$ denotes the limit as $n \rightarrow \infty$ of the family of n -vertex graphs of type G .

This limit has some characteristics in common with the thermodynamic limit in statistical mechanics, in which one defines a partition function at a given temperature T and external field H as $Z = \sum_{\{\sigma_i\}} e^{-\beta \mathcal{H}}$ (where the Hamiltonian \mathcal{H} describes the interactions of the spins σ_i , and $\beta = (k_B T)^{-1}$) and then, starting with a finite, usually regular, d -dimensional n -vertex lattice $G = \Lambda$ with some specified boundary conditions, one considers the reduced free energy (per site) f in the thermodynamic limit,

$$e^f = \lim_{n \rightarrow \infty} Z^{1/n} \quad (1.2)$$

(Here, f is related to the actual free energy F by $f = -\beta F$.) For spin models in the physical temperature range, $0 \leq \beta \leq \infty$, the partition function Z is positive. In the case of the chromatic polynomial, for sufficiently large q , $P(G, q) > 0$. In both cases, one naturally chooses the real positive $1/n$ 'th roots in the respective eqs. (1.1) and (1.2).

Although the number of colors q is an integer in the initial mathematical definition of the chromatic polynomial, one may generalize q to a real or, indeed, complex variable. We shall consider this generalization here and study the function $W(\{G\}, q)$ and the related zeros of $P(G, q)$ in the complex q plane for various families of graphs G . For certain ranges of real q , $P(G, q)$ can be negative, and, of course, when q is complex, so is $P(G, q)$ in general. In these cases it may not be obvious, *a priori*, which of the n roots

$$P(G, q)^{1/n} = \{|P(G, q)|^{1/n} e^{2\pi i r/n}\}, \quad r = 0, 1, \dots, n-1 \quad (1.3)$$

to choose in eq. (1.1). Consider the function $W(\{G\}, q)$ defined via eq. (1.1) starting with q on the positive real axis where $P(G, q) > 0$, and consider the maximal region in the complex

q plane which can be reached by analytic continuation of this function. We denote this region as R_1 . Clearly, the phase choice in (1.3) for $q \in R_1$ is that given by $r = 0$, namely $P(G, q)^{1/n} = |P(G, q)|^{1/n}$. However, as we shall see via exactly solved cases, there can also be families of graphs $\{G\}$ for which the analytic structure of $W(\{G\}, q)$ includes other regions not analytically connected to R_1 , and in these regions, there may not be any canonical choice of phase in (1.3). We shall discuss this further below.

Besides being of interest in mathematics, chromatic polynomials $P(G, q)$ and their asymptotic limits $W(\{G\}, q)$ have a deep connection with statistical mechanics, specifically, the Potts antiferromagnet (AF) [6]-[9]. Denote the partition function for the (isotropic, nearest-neighbor, zero-field) q -state Potts model at a temperature T as $Z = \sum_{\{\sigma_n\}} e^{-\beta\mathcal{H}}$ with the Hamiltonian

$$\mathcal{H} = -J \sum_{\langle ij \rangle} \delta_{\sigma_i \sigma_j} \quad (1.4)$$

where $\sigma_i = 1, \dots, q$ are Z_q -valued variables on each site $i \in \Lambda$. Define

$$K = \beta J, \quad a = e^K \quad (1.5)$$

For the Potts antiferromagnet ($J < 0$), in the limit $T \rightarrow 0$, i.e., $K \rightarrow -\infty$, the partition function only receives nonzero contributions from spin configurations in which $\sigma_i \neq \sigma_j$ for nearest-neighbor vertices i and j , and hence, formally,

$$Z(\Lambda, q, K = -\infty) = P(\Lambda, q) \quad (1.6)$$

whence

$$\exp(f(\Lambda, q, K = -\infty)) = W(\Lambda, q) \quad (1.7)$$

where $G = \Lambda$ denotes the lattice.

However, as we shall discuss in detail, the limit (1.1), and hence the resultant function $W(\{G\} = \Lambda, q)$ is not well-defined at certain special points q_s without specifying further information. This constitutes a fundamental difference between the limits (1.1) and (1.2); in statistical mechanics, if the point K_0 lies within the interior of a given physical phase, then $f(\Lambda, K)$ is a (real) analytic function of K . Furthermore, in statistical mechanics the limit $K \rightarrow K_0$ for a physical K , and the thermodynamic limit $n \rightarrow \infty$ (with the d -dimensional volume $vol_d(\Lambda) \rightarrow \infty$) commute [10]

$$\lim_{n \rightarrow \infty} \lim_{K \rightarrow K_0} Z^{1/n} = \lim_{K \rightarrow K_0} \lim_{n \rightarrow \infty} Z^{1/n} \quad (1.8)$$

These limits still commute for complex K . In contrast, the definition of $W(\Lambda, q)$ involves a further subtlety, since at certain special points q_s the following limits do *not* commute (for

any choice of r in eq. (1.3)):

$$\lim_{n \rightarrow \infty} \lim_{q \rightarrow q_s} P(G, q)^{1/n} \neq \lim_{q \rightarrow q_s} \lim_{n \rightarrow \infty} P(G, q)^{1/n} \quad (1.9)$$

As we shall discuss, the origin of this noncommutivity of limits is an abrupt change in the behavior of $P(G, q)$ in the vicinity of such a point q_s ; for $q \neq q_s$, $P(G, q)$ grows exponentially as the number of vertices n in G goes to infinity: $P(G, q) \sim a^n$ for some nonzero a , whereas precisely at $q = q_s$, it has a completely different type of behavior, which, in all of the cases considered here is either $P(G, q_s) = c_0(q_s)$ where $c_0(q)$ may be a constant, independent of n or may depend on n in a way that does not involve exponential growth, like $(-1)^n$. The set of special points $\{q_s\}$ includes $q = 0$, $q = 1$, and, on any graph G which contains at least one triangle, also $q = 2$; at these points, $P(G, q_s) = 0$. It is also possible for $P(G, q_s)$ to be equal to a nonzero constant at q_s . We shall discuss this further in Section 2.

Before proceeding, we mention that, in addition to Refs. [1]-[4], some relevant previous works are Refs. [11]-[14]. In particular, in Refs. [13, 14], Baxter gave exact results for $W(\text{tri}, q)$ on the triangular (*tri*) lattice, and determined its analytic structure in the complex q plane.

This paper is organized as follows. In Section 2 we discuss a subtlety in the definition of $W(\{G\}, q)$, and in Section 3 we present some general results on the analytic structure of this function in the complex q plane. In Section 4 we give a number of exact solutions for $W(\{G\}, q)$ for various families of graphs $\{G\}$ and calculate the resultant diagrams, showing the analytic structure of $W(\{G\}, q)$ in the complex q plane. Section 5 contains a discussion of zeros of chromatic polynomials for various families of graphs and, in particular, a theorem on the location and density of zeros of $P(G, q)$ for certain families G . In Section 6 we present a theorem specifying the maximal value of q , for a given lattice Λ , where the region boundary \mathcal{B} for $W(\Lambda, q)$ crosses the real q axis, and we apply this to specific lattices. Section 7 gives numerical calculations of $W(\Lambda, q)$ for the honeycomb and square lattices and a comparison with large- q series. Section 8 contains some concluding remarks.

2 On the Definition of $W(\{G\}, q)$

In order to discuss the subtlety in the definition of $W(\{G\}, q)$, we first recall the following general properties concerning the zeros of chromatic polynomials. First, for any graph G ,

$$P(G, q = 0) = 0 \quad (2.1)$$

Second, for any graph G consisting of at least two vertices (with a bond connecting them),

$$P(G, q = 1) = 0 \quad (2.2)$$

Third, for any graph G containing at least one triangle,

$$P(G, q = 2) = 0 \quad \text{if} \quad G \supseteq \triangle \quad (2.3)$$

These properties are obvious from the definition of $P(G, q)$, given that one must color adjacent vertices with different colors. Since $P(G, q)$ is a polynomial, each of these zeros at the respective values $q_0 = 0, 1$ or 2 means that $P(G, q)$ must factorize according to

$$P(G, q) = (q - q_0)^{b(q_0)} Q(G, q) \quad (2.4)$$

where $b(q_0)$ is a positive integer and $Q(G, q_0) \neq 0$. One may distinguish two particular cases that occur for cases we have studied: (i) $b(q_0) = b_0 + b_1 n$; (ii) $b(q_0) = b_0$, where b_0 and b_1 are integers independent of n . In the first, case,

$$W(\{G\}, q) = (q - q_0)^{b_1} \lim_{n \rightarrow \infty} Q(\{G\}, q)^{1/n} \quad (2.5)$$

so that the two different orders of limits in (1.9) do commute. This type of behavior is observed for tree graphs, our first example below. However, in all of the other cases which we have studied, the second type of behavior (ii) holds. Hence for these families of graphs, as a consequence of the basic fact that

$$\lim_{n \rightarrow \infty} x^{1/n} = \begin{cases} 1 & \text{if } x \neq 0 \\ 0 & \text{if } x = 0 \end{cases} \quad (2.6)$$

and hence, $\lim_{n \rightarrow \infty} \lim_{q \rightarrow q_0} (q - q_0)^{b(q_0)/n} = 0$ and $\lim_{q \rightarrow q_0} \lim_{n \rightarrow \infty} (q - q_0)^{b(q_0)/n} = 1$, the noncommutativity of the limits in eq. (1.9) follows (for any value of r in (1.3)):

$$\lim_{n \rightarrow \infty} \lim_{q \rightarrow q_0} P(G, q)^{1/n} = 0 \quad (2.7)$$

whereas

$$\lim_{q \rightarrow q_0} \lim_{n \rightarrow \infty} P(G, q)^{1/n} = \lim_{q \rightarrow q_0} \lim_{n \rightarrow \infty} Q(G, q)^{1/n} \neq 0 \quad (2.8)$$

More generally, eq. (1.1) is insufficient to define $W(\{G\}, q)$ not just in the vicinity of a zero of $P(G, q)$, but also in the vicinity of any special point q_s where the asymptotic behavior of $P(G, q)$ changes abruptly from

$$P(G, q) \sim a^n \quad \text{as} \quad n \rightarrow \infty \quad (2.9)$$

with a a nonzero constant, to

$$P(G, q_s) = \text{const.} \quad \text{as} \quad n \rightarrow \infty \quad (2.10)$$

In case (ii) of eq. (2.4), with $b(q_s) = b_0$, one encounters this type of abrupt change in behavior with the constant in eq. (2.10) equal to zero. This is the origin of the noncommutativity of limits in eq. (1.9) at $q = 0, 1$ and, for $G \supseteq \Delta$, at $q = 2$. However, this noncommutativity is more general and can also occur when the constant in eq. (2.10) is nonzero. An example is provided by the point $q_s = 3$ on the triangular lattice; there are $3! = 6$ ways of coloring a triangular lattice graph (with the technical provision that for finite triangular lattice graphs, one uses boundary conditions which do not introduce frustration). Denoting such a triangular lattice graph as tri_n , it follows that $P(tri_n, 3) = 6$, which is of the form of eq. (2.10) with a nonzero constant. For such cases, where the constant in eq. (2.10) is nonzero, one has

$$\lim_{n \rightarrow \infty} \lim_{q \rightarrow q_s} |P(G, q)|^{1/n} = 1 \quad (2.11)$$

while

$$\lim_{q \rightarrow q_s} \lim_{n \rightarrow \infty} |P(G, q)|^{1/n} = |a| \quad (2.12)$$

where, in general, $a \neq 1$. Finally, the set of points $\{q_s\}$ also may include a continuous set comprising part of a region boundary, as will be discussed in theorem 1, part (e) below.

Because of the noncommutativity (1.9), the formal definition (1.1) is, in general, insufficient to define $W(\{G\}, q)$ at the set of special points $\{q_s\}$; at these points, one must also specify the order of the limits in (1.9). One can maintain the analyticity of $W(\{G\}, q)$ at these special points q_s of $P(G, q)$ by choosing the order of limits in the right-hand side of eq. (1.9):

$$W(\{G\}, q_s)_{D_{qn}} \equiv \lim_{q \rightarrow q_s} \lim_{n \rightarrow \infty} P(G, q)^{1/n} \quad (2.13)$$

As indicated, we shall denote this definition as D_{qn} , where the subscript indicates the order of the limits. Although this definition maintains the analyticity of $W(\{G\}, q)$ at the special points q_s , it produces a function $W(\{G\}, q)$ whose values at the points q_s differ significantly from the values which one would get for $P(G, q_s)^{1/n}$ with finite- n graphs G . The definition based on the opposite order of limits,

$$W(\{G\}, q_s)_{D_{nq}} \equiv \lim_{n \rightarrow \infty} \lim_{q \rightarrow q_s} P(G, q)^{1/n} \quad (2.14)$$

gives the expected results like $W(G, q_s) = 0$ for $q_s = 0, 1$, and, for $G \supseteq \Delta$, $q = 2$, as well as $W(tri_n, q = 3) = 1$, but yields a function $W(\{G\}, q)$ with discontinuities at the set of points $\{q_s\}$. In our results below, in order to avoid having to write special formulas for the points q_s , we shall adopt the definition D_{qn} but at appropriate places will take note of the noncommutativity of limits (1.9).

As noted in the introduction, the noncommutativity of limits (1.9) and resultant subtlety in the definition of $W(\{G\}, q)$ is fundamentally different from the behavior of the (otherwise

somewhat analogous) function $e^{f(G,K)}$ in statistical mechanics (where for this discussion, we consider a general statistical mechanical model and its reduced free energy, f , and do not restrict to the Potts model). The set $\{q_s\}$ includes certain discrete points lying within regions in the complex q plane where $W(\{G\}, q)$ is otherwise an analytic function. Now, considering the thermodynamic limit of a statistical mechanical model on a lattice $G = \Lambda$, one knows that for physical K , after the additive term $(\zeta/2)K + h$ is removed (where ζ is the coordination number of the lattice Λ , $h = \beta H$, and this removes the trivial isolated infinities in f at $K = \infty$ and $h = \infty$), i.e. after defining $f(\Lambda, K) = (\zeta/2)K + h + f_r(\Lambda, K)$, the function $f_r(\Lambda, K)$ is analytic within the interior of a given phase. We should remark that in our studies of the properties of spin models generalized to complex-temperature, we have established that there may be singularities in thermodynamic quantities in the interiors of (complex-temperature extensions of physical) phases; specifically, we proved a theorem (theorem 6 in Ref. [15]) that on a lattice with odd coordination number, the zero-field Ising model partition function vanishes, and the free energy f has a negatively divergent singularity, at the complex-temperature point $z = -1$, where $z = e^{-2K_I}$ and $K_I = \beta J_I$ is the Ising spin-spin coupling. For the honeycomb lattice, $z = -1$ lies on a phase boundary [43], but for the heteropolygonal lattice denoted $3 \cdot 12^2$, $z = -1$ lies in the interior of the complex-temperature extension of the ferromagnetic phase [15]. However, in the quantity analogous to $W(\Lambda, q)$, namely, $e^{f(\Lambda, K)}$, this singularity is a zero, not a discontinuity and furthermore it is not associated with the type of noncommutativity analogous to (1.9). The reason for this is that when one factorizes the (zero-field) partition function in a manner similar to eq. (2.4),

$$Z(\Lambda, z) = (z + 1)^{n/2} Z_s(\Lambda, z) \quad (2.15)$$

(which defines $Z_s(\Lambda, z)$), the exponent of the factor $(z + 1)$ is proportional to n , as in case (i) for eq. (2.4), so that the following limits commute:

$$\lim_{z \rightarrow -1} \lim_{n \rightarrow \infty} Z(\Lambda_n, z) = \lim_{n \rightarrow \infty} \lim_{z \rightarrow -1} Z(\Lambda_n, z) = 0 \quad (2.16)$$

One should also contrast the noncommutativity (1.9) with the very different type of noncommutativity which applies to a symmetry-breaking order parameter such as a (uniform or staggered) magnetization in a statistical mechanical spin model (above its lower critical dimensionality, so that it has a symmetry-breaking phase transition). Here, in both the symmetric, high-temperature phase and the low-temperature phase with spontaneously broken symmetry, if one removes the external field before taking the thermodynamic limit, the magnetization vanishes:

$$\lim_{n \rightarrow \infty} \lim_{H \rightarrow 0} M(\Lambda, K, H) = 0 \quad (2.17)$$

whereas in the low-temperature, symmetry-broken phase ($K > K_c$), there is a nonzero magnetization in the thermodynamic limit:

$$\lim_{H \rightarrow 0} \lim_{n \rightarrow \infty} M(\Lambda, K, H) \neq 0, \quad \text{for } K > K_c \quad (2.18)$$

However, this noncommutativity is quite different from that in eq. (1.9): this is clear from the fact that, among other things, (1.9) can occur at a discrete, isolated set of special points q_s (as well as possibly a continuous set on a region boundary of type (e) in theorem 1 below), whereas the noncommutativity in eqs. (2.17), (2.18) occurs throughout the low-temperature, broken-symmetry phase of the spin model and, indeed, can be used to characterize this phase, with the spontaneous magnetization $M(K, 0)$ (defined of course by the second ordering of limits, (2.18)) constituting the order parameter.

3 Analytic Structure of $W(\{G\}, q)$

As noted, we shall consider the variable q to be extended from the positive integers to the complex numbers. Although for a given graph G , $P(G, q)$ is a polynomial and hence, *a fortiori*, is an analytic function of q , the function $W(\{G\}, q)$ which describes the $n \rightarrow \infty$ limit of a given family of graphs $\{G\}$ will, in general, fail to be analytic at certain points. These points may form a discrete or continuous set; if the set is continuous, it may separate certain regions of the complex q plane, which we denote R_i . We shall denote the boundary separating regions R_i and R_j as $\mathcal{B}(R_i, R_j)$ and the union of all components of regional boundaries as $\mathcal{B} = \cup_{i,j} \mathcal{B}(R_i, R_j)$. On these boundaries, $W(\{G\}, q)$ is non-analytic. We shall illustrate this with exact results below. These regions are somewhat similar to complex-temperature extensions or complex-field extensions of physical phases in statistical mechanical models. However, there are also some fundamental differences. One of these is the noncommutativity of limits discussed in the previous section. Another is that in the case of $W(\{G\}, q)$, it is not clear what would play the role of the physical concept of a order parameter characterizing a given phase (and its complex extension, such as to complex-temperature). Therefore, we shall use the terms “region” and “region diagram” rather than (complex extensions of) “phase” and “phase diagram”.

A question that arises when one considers the somewhat related regions (phases) in complex-temperature or complex-field variables for statistical mechanical spin models concerns the dimensionality of the locus of points where the reduced free energy f is non-analytic. Where the premise of the Yang-Lee theorem [19] holds (i.e., for physical temperature and Hamiltonians with ferromagnetic, but not necessarily nearest-neighbor, two-spin interactions, $\mathcal{H} = -\sum_{\langle ij \rangle} \sigma_i J_{ij} \sigma_j - H \sum_i \sigma_i$ on arbitrary graphs), it states that the zeros of Z in the

complex $\mu = e^{-2\beta H}$ plane lies on the unit circle $|\mu| = 1$ and hence, in the thermodynamic limit where these merge to form the continuous locus of points where f is non-analytic in the μ plane, this locus is one-dimensional. In the case of complex-temperature, taking the Ising model for illustration, the locus of points in the $z = e^{-2K}$ plane is usually one-dimensional for isotropic spin-spin couplings J , but on the heteropolygonal $4 \cdot 8^2$ lattice, it fills a two-dimensional area in this plane even for isotropic couplings [15]. In all of the exact results for $W(\{G\}, q)$ that we shall present below, the dimension of the continuous locus of points where $W(\{G\}, q)$ is non-analytic, is $\dim\{\mathcal{B}\} = 1$.

We next present a general theorem.

Theorem 1

Let G be a graph with n vertices and suppose that $P(G, q)$ has the form

$$P(G, q) = q(q-1) \left\{ c_0(q) + \sum_{j=1}^{N_a} c_j(q) a_j(q)^n \right\} \quad (3.1)$$

where $c_j(q)$ are polynomials in q . Here $c_0(q)$ may contain n -dependent terms, such as $(-1)^n$, but does not grow with n like a^n . This form and the additional factorization (3.4) are motivated by the exact solutions to be presented below. Note that the fact that $P(G, q)$ is a polynomial guarantees that, for a given G , N_a is finite. For a fixed q and, more generally, for a given region in the complex q plane, we define a term $a_\ell(q)$ to be leading if for q in this region $|a_\ell(q)| \geq 1$ and $|a_\ell(q)| > |a_j(q)|$ for all $j \neq \ell$. Without loss of generality, we can write (3.1) so that the $a_j(q)$ are different functions of q . Then our theorem states that (a) if $N_a \geq 2$ and there exists some ℓ such that $|a_\ell(q)| > 1$ in a given region of the complex q plane, then if in this region, $|a_j(q)| < 1$, the term $a_j(q)$ does not contribute to the limiting function $W(G, q)$; (b) if $N_a = 1$ and $c_0(q) \neq 0$, then if $|a_1| < 1$, this term again does not contribute to $W(G, q)$, which is then determined by $c_0(q)$; (c) if $N_a \geq 1$ and $a_\ell(q)$ is a leading term in a given region of the q plane then (i) if this region is analytically connected to the positive real axis where $P(G, q) > 0$ so that $r = 0$ in (1.3),

$$W(\{G\}, q) = a_\ell(q) \quad (3.2)$$

while (ii) if (i) is not the case, then at least in terms of magnitudes, one has the result

$$|W(\{G\}, q)| = |a_\ell(q)| \quad (3.3)$$

(d) the regional boundaries \mathcal{B} separating regions where different leading terms dominate are determined by the degeneracy in magnitude of these leading terms: $|a_\ell(q)| = |a_{\ell'}(q)|$; (e) a

regional boundary can also occur where one crosses from a region where there is a leading term $a_\ell(q)$ to one where there is no leading term but there is a nonzero $c_0(q)$; this type of boundary is given by the equation $|a_\ell(q)| = 1$.

Proof: (a) is clear since if $|a_j(q)| < 1$, then $\lim_{n \rightarrow \infty} a_j(q)^n = 0$, so in this limit it does not contribute to $W(G, q)$, which is determined by the leading term, as specified in part (c). Part (b) follows by the same type of logic. Note that if there is no $c_0(q)$ term and if $N_a = 1$ with $|a_1(q)| < 1$, then in this case, a_1 still determines $W(G, q)$; an example of this is provided by the region $|q - 1| < 1$ for the tree graphs T_n to be discussed below. Part (c) expresses the fact that in the limit $n \rightarrow \infty$, the contributions of subleading terms are negligible relative to that of the leading term, and hence the limiting function $W(\{G\}, q)$ depends only on this leading term. As one moves from a region with one dominant term $a_\ell(q)$ to a region in which a different term $a_{\ell'}(q)$ dominates, there is a non-analyticity in $W(\{G\}, q)$ as it switches from $W(\{G\}, q) = a_\ell(q)$ to $W(\{G\}, q) = a_{\ell'}(q)$ for $r = 0$ and similarly for nonzero r . This also proves (d). Statement (e) follows in a similar way.

It is possible that $P(G, q)$ contains no term of the form $c_j(q)a_j(q)^n$ but instead only the term $c_0(q)$. Moreover, in the case where $P(G, q)$ does contain such $c_j(q)a_j(q)^n$ terms, there may exist a region in the q plane where $|a_j(q)| < 1$ for all $j = 1, \dots, N_a$. In both of these cases, $W(\{G\}, q)$ is determined by the remaining function $c_0(q)$.

If G contains one or more triangles Δ , then one may express $P(G, q)$ in the form

$$P(G, q) = q(q-1)(q-2) \left\{ c_0(q) + \sum_{j=1}^{N_a} c_j(q)a_j(q)^n \right\} \quad \text{if } G \supseteq \Delta \quad (3.4)$$

In this case, the same theorem applies, but with the further factorization (3.4) taken into account.

The subtlety in the definition of $W(\{G\}, q)$ resulting from the noncommutativity (1.9) is evident in the forms (3.1) and (3.4). With the definition (2.13), if there is a leading term a_ℓ at $q_0 = 0, 1$, and, for $\{G\} \supseteq \Delta$, also $= 2$, then

$$|W(\{G\}, q_0)| = |a_\ell(q_0)| \quad (3.5)$$

rather than zero, even though $P(G, q_0) = 0$ at these points. If there is no leading term in the vicinity of a given q_0 , i.e., if $|a_j(q_0)| < 1$ for all $j = 1, \dots, N_a$, then

$$\begin{aligned} |W(\{G\}, q)| &= \lim_{n \rightarrow \infty} \lim_{q \rightarrow q_0} |c_0(q)|^{1/n} \\ &= \begin{cases} 1 & \text{if } |c_0(q_0)| \neq 0 \\ 0 & \text{if } c_0(q_0) = 0 \end{cases} \end{aligned} \quad (3.6)$$

4 Exact Solutions for $W(\{G\}, q)$

In this section we calculate and discuss exact solutions for $W(\{G\}, q)$ for various families $\{G\}$ of graphs. We believe that these give some interesting insights into the analytic properties of such functions and also into the exact results obtained by Baxter for the triangular lattice. Unless otherwise cited, chromatic polynomials can be found, together with further properties of graphs, in Refs. [4]-[5].

4.1 Tree Graphs

A tree graph T_n is an n -vertex graph with no circuits and has the chromatic polynomial $P(T_n, q) = q(q-1)^{n-1}$. Using the procedure discussed in section 2, we choose $r = 0$ in (1.3) and obtain

$$W(\{T\}, q) = q - 1 \quad (4.1.1)$$

This applies for all q ; i.e., $W(\{T\}, q)$ is analytic throughout the entire (finite) complex q plane.

4.2 Complete Graphs

An n -vertex graph is termed “complete” and denoted K_n if each vertex is completely connected by bonds (edges) with all the other vertices. Thus, K_3 is the triangle, K_4 the tetrahedron, and so forth. The chromatic polynomial is $P(K_n, q) = \prod_{i=0}^{n-1} (q-i)$. For a given n , we may choose $r = 0$ in (1.3) by starting on the positive real q axis at a value $q > n - 1$. This yields

$$W(\{K\}, q) = 1 \quad (4.2.1)$$

With our definition (2.13), $W(\{K\}, q)$ is analytic in the entire (finite) q plane. The zeros of $P(K_n, q)$ are comprised by the set $\{q_0\} = \{0, 1, \dots, n-1\}$ and the noncommutativity of limits (1.9) occurs at each of these points.

4.3 Cyclic Graphs

For the cyclic graph C_n , i.e., the n -circuit, the chromatic polynomial is $P(C_n, q) = (q-1)\{(q-1)^{n-1} + (-1)^n\}$. We find that the analytic structure of $W(\{C\}, q)$ differs in the two regions R_1 and R_2 consisting of q satisfying $|q-1| > 1$ and $|q-1| < 1$, respectively. The boundary \mathcal{B} separating these regions is thus the unit circle centered at $q = 1$. These regions are shown in Fig. 1. We calculate

$$W(\{C\}, q) = q - 1 \quad \text{for } q \in R_1 \quad (4.3.1)$$

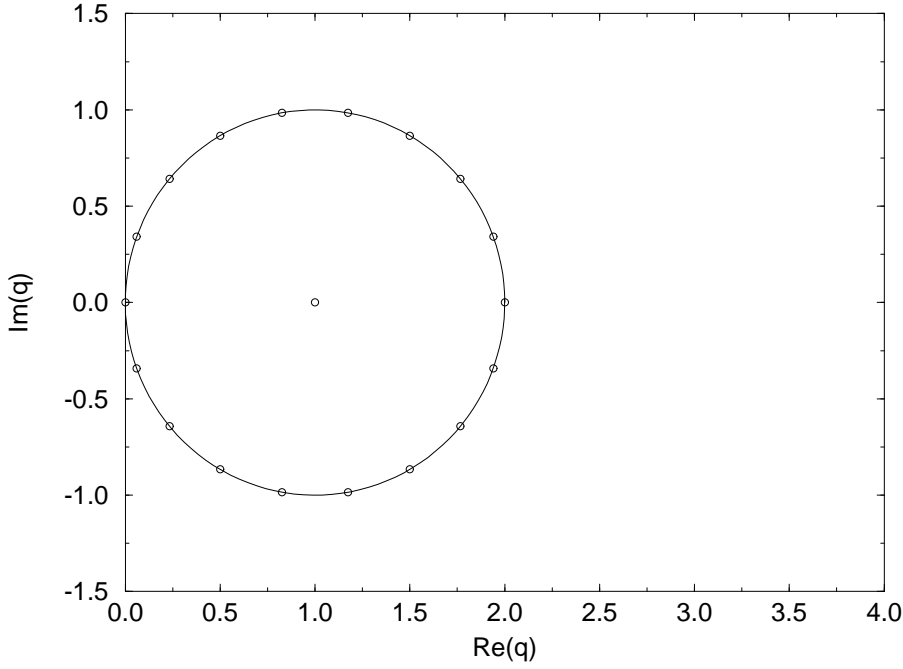


Figure 1: Diagram showing regional boundaries comprising \mathcal{B} for $W(\{C\}, q)$ for cyclic graphs and zeros of $P(C_n, q)$ for $n = 19$.

For $q \in R_2$, the first term in curly brackets, $(q-1)^{n-1} \rightarrow 0$ as $n \rightarrow \infty$, and hence $P(C_n, q) \rightarrow (q-1)(-1)^n$. This function does not have a limit as $n \rightarrow \infty$. However, we can observe that

$$|W(\{C\}, q)| = 1 \quad \text{for } q \in R_2 \quad (4.3.2)$$

$|W(\{C\}, q)|$ is, in general, discontinuous along \mathcal{B} . For the choice $r = 0$ in (1.3), it is continuous at $q = 2$ and has a discontinuity of

$$\lim_{q \searrow 0} W(\{C\}, q) - \lim_{q \nearrow 0} W(\{C\}, q) = 2 \quad (4.3.3)$$

at $q = 0$. In Fig. 1 we have also plotted the zeros of $P(C_n, q)$ for a typical value, $n = 19$. These will be discussed in Section 5.

4.4 Wheel Graphs

The wheel graph $(Wh)_n$ is defined as an $(n-1)$ -circuit C_{n-1} with an additional vertex joined to all of the $n-1$ vertices of C_{n-1} (which can be thought of as the center of the wheel), and is naturally defined for $n \geq 3$. We find that the diagram describing the analytic structure of $W(\{Wh\}, q)$ consists of the two regions R_1 and R_2 defined respectively by $|q-2| > 1$ and $|q-2| < 1$, with the boundary \mathcal{B} consisting of the unit circle $|q-2| = 1$. (These R_1 and R_2 should not be confused with the regions discussed in the previous subsection; we define the regions R_j differently for each family of graphs.) This diagram is thus similar to Fig. 1 but with the circle moved one unit to the right; for brevity we do not show it. Using

$$P((Wh)_n, q) = q(q-2)\{(q-2)^{n-2} - (-1)^n\} \quad (4.4.1)$$

we calculate

$$W(\{Wh\}, q) = q-2 \quad \text{for } q \in R_1 \quad (4.4.2)$$

For $q \in R_2$, since the first term in curly brackets in eq. (4.4.1), $(q-2)^{n-2}$, goes to zero as $n \rightarrow \infty$, one is left only with the second term, $-(-1)^n$; this term does not have a smooth limit as $n \rightarrow \infty$ and hence neither does the $1/n$ 'th power of this quantity. However, $|W(\{Wh\}, q)| = 1$ for $q \in R_2$. Formally, one may choose the $1/n$ 'th root such that $W(\{Wh\}, q) = -1$ for $q \in R_2$. The noncommutativity of limits in eq. (1.9) occurs at the discrete points $q = 0, 1, 2$ and, for even n , also at $q = 3$ since $P((Wh)_n, n \text{ even}, q = 3) = 0$. More generally, this noncommutativity occurs along the circle $|q-2| = 1$.

One can also study wheel graphs with some spokes removed, which have been of recent interest [16]. Let us define the ‘‘cut’’ wheel $(cWh)_{n,\ell}$ as the n -vertex wheel graph with ℓ consecutive spokes removed. For example, from an analysis of the specific case $\ell = 2$, we find the same boundary \mathcal{B} , $|q-2| = 1$, as for the asymptotic limit of the wheel graphs, and, furthermore, $W(\{cWh\}, q) = W(\{Wh\}, q)$.

4.5 Biwheel Graphs

The biwheel graph U_n is defined by adjoining a second vertex to all of the other vertices in the wheel graph $(Wh)_{n-1}$ and is naturally defined for $n \geq 4$. Here, we find that the diagram describing the analytic structure of $W(\{U\}, q)$ consists of the two regions R_1 and R_2 defined respectively by $|q-3| > 1$ and $|q-3| < 1$ with \mathcal{B} consisting of the circle $|q-3| = 1$. The chromatic polynomial for these graphs is

$$P(U_n, q) = q(q-1)(q-3)\{(q-3)^{n-3} + (-1)^n\} \quad (4.5.1)$$

and from this we calculate

$$W(\{U\}, q) = q - 3 \quad \text{for } q \in R_1 \quad (4.5.2)$$

For $q \in R_2$, the term $(q-3)^{n-3} \rightarrow 0$ as $n \rightarrow \infty$, and one is again left with a discontinuous term $(-1)^n$. As before, one has in general, that for $q \in R_2$, $|W(\{U\}, q)| = 1$, and one can formally choose the $1/n$ 'th root such that $W(\{U\}, q) = -1$ in this region. The noncommutativity of limits in (1.9) occurs at the discrete points $q = 0, 1, 2, 3$, and also, if n is odd, at $q = 4$ since $P(U_n, n \text{ odd}, q = 4) = 0$; more generally, it occurs on the circle $|q - 3| = 1$.

4.6 Bipyrmaid Graphs

The bipyrmaid B_n is formed from the biwheel U_n by removing the bond connecting the adjoined vertex to the center vertex of the biwheel. A bipyrmaid graph can be inscribed on the 2-sphere S^2 and, in this sense, can be considered to be 2-dimensional. The chromatic polynomial for B_n is

$$P(B_n, q) = q \left\{ (q-2)^{n-2} + (q-1)(q-3)^{n-2} + (-1)^n (q^2 - 3q + 1) \right\} \quad (4.6.1)$$

Here we find a more complicated diagram describing the analytic structure; this is shown in Fig. 2 and consists of three regions:

$$R_1 : \operatorname{Re}(q) > \frac{5}{2} \quad \text{and} \quad |q - 2| > 1 \quad (4.6.2)$$

$$R_2 : \operatorname{Re}(q) < \frac{5}{2} \quad \text{and} \quad |q - 3| > 1 \quad (4.6.3)$$

and

$$R_3 : |q - 2| < 1 \quad \text{and} \quad |q - 3| < 1 \quad (4.6.4)$$

The boundaries between these regions are thus the two circular arcs

$$\mathcal{B}(R_1, R_3) : q = 2 + e^{i\theta}, \quad -\frac{\pi}{3} < \theta < \frac{\pi}{3} \quad (4.6.5)$$

and

$$\mathcal{B}(R_2, R_3) : q = 3 + e^{i\phi}, \quad \frac{2\pi}{3} < \phi < \frac{4\pi}{3} \quad (4.6.6)$$

together with the semi-infinite vertical line segments

$$\mathcal{B}(R_1, R_2) = \{q\} : \operatorname{Re}(q) = \frac{5}{2} \quad \text{and} \quad |\operatorname{Im}(q)| > \frac{\sqrt{3}}{2} \quad (4.6.7)$$

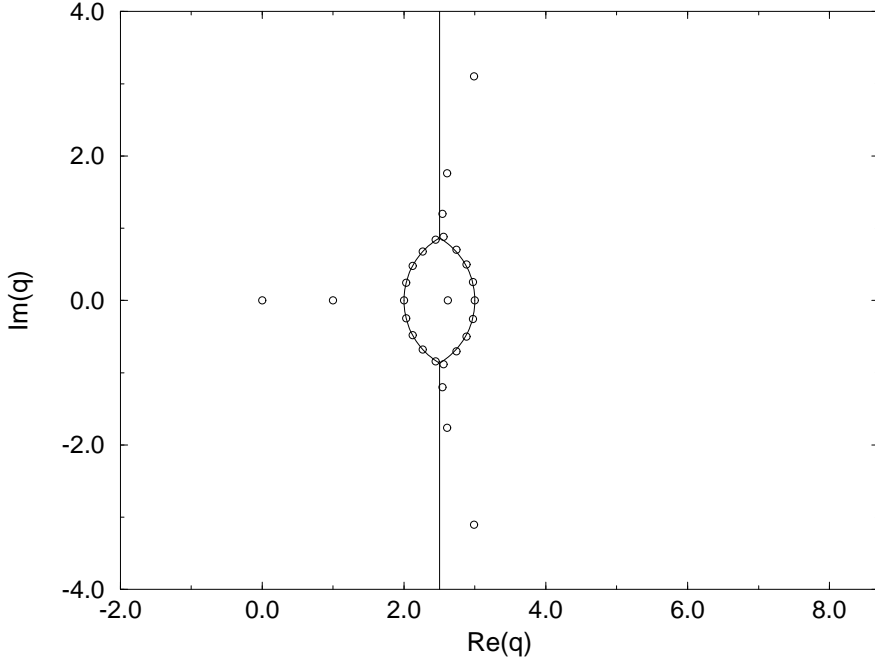


Figure 2: Diagram showing regional boundaries comprising \mathcal{B} for $W(\{B\}, q)$ for bipyramid graphs and zeros of $P(B_n, q)$ for $n = 29$.

These meet at the intersection points $q = 5/2 \pm i\sqrt{3}/2$. We find that

$$W(\{B\}, q) = q - 2 \quad \text{for } q \in R_1 \quad (4.6.8)$$

For the other regions, we have, in general,

$$\begin{aligned} |W(\{B\}, q)| &= |q - 3| \quad \text{for } q \in R_2 \\ &= 1 \quad \text{for } q \in R_3 \end{aligned} \quad (4.6.9)$$

With specific choices of $1/n$ 'th roots, one can choose $W(\{B\}, q) = q - 3$ in R_2 and -1 in R_3 .

This example provides an illustration of the noncommutativity of limits (1.9) for a real non-integer point q_0 , namely, $q_0 = (1/2)(3 + \sqrt{5}) = Be_5 = 2.618\dots$, where the r 'th Beraha number Be_r is given by [18]

$$Be_r = 4 \cos^2(\pi/r) \quad (4.6.10)$$

for $r = 1, 2, \dots$. The point Be_5 lies in the region R_3 where $q^2 - 3q + 1$ is the dominant term and is one of the two roots of this polynomial (the other root lies in region R_2 and hence plays no role in $W(\{B\}, q)$). In Fig. 2 we have also plotted zeros of the bipyramid chromatic polynomial $P(B_n, q)$ for a typical finite $n = 29$. These will be discussed in Section 5.

Since $W(\{G\}, q)$ is bounded above by q , it is common to remove this factor and define a reduced function

$$W_r(\{G\}, q) = q^{-1}W(\{G\}, q) \quad (4.6.11)$$

which has a finite limit as $|q| \rightarrow \infty$. There have been a number of calculations of Taylor series expansions in the variable $1/(q-1)$ for functions equivalent to W_r in the case where G is a regular lattice; see, for example, Ref. [20] (and earlier references therein) for the square, triangular, and honeycomb lattices. Clearly, these series expansions rely on the property that, for these lattices, $W_r(\{G\}, q)$ is an analytic function in the $1/q$ plane at the origin, $1/q = 0$. This analyticity of $W(\Lambda, q)$ at $1/q = 0$ is proved by exact results for the triangular lattice and is strongly supported by numerical calculations of zeros of $P(\Lambda, q)$ for $\Lambda = sq, hc$ [14], which show that the respective regional boundaries for these three lattices are compact, and do not extend to infinite distance from the origin in the complex q plane. However, our exact result for the infinite- n bipyramid function $W(\{B\}, q)$ and its region diagram demonstrates that, in general, the infinite- n limit $W(\{G\}, q)$ of chromatic polynomials for a given family of graphs $\{G\}$ is *not* guaranteed to be analytic at $1/q = 0$: in the case of the bipyramid graphs, the portion of the regional boundary \mathcal{B} comprised by the line segment (4.6.7) runs vertically through the origin of the $1/q$ plane, and $W(\{B\}, q)$ is not analytic at $1/q = 0$.

4.7 Cyclic Ladder Graphs L_{2n}

The cyclic ladder graphs with $2n$ vertices can be visualized as two n -circuit graphs (rings) C_n , one above the other, with the i 'th vertex of one n -circuit connected by a vertical bond to the i 'th vertex of the other n -circuit. The chromatic polynomial for this family of graphs was calculated in Ref. [17] (where they are called prism graphs):

$$P(L_{2n}, q) = (q^2 - 3q + 3)^n + (q - 1)\{(3 - q)^n + (1 - q)^n\} + q^2 - 3q + 1 \quad (4.7.1)$$

From this we compute the region diagram shown in Fig. 3, consisting of four regions: R_1 , R_2 , R_2^* , and R_3 in which, respectively, (1) $(q^2 - 3q + 3)^n$, (2)-(2)* $(1 - q)^n$, and (3) $(3 - q)^n$ are the leading terms. We find

$$W(\{L\}, q) = q^2 - 3q + 3 \quad \text{for } q \in R_1 \quad (4.7.2)$$

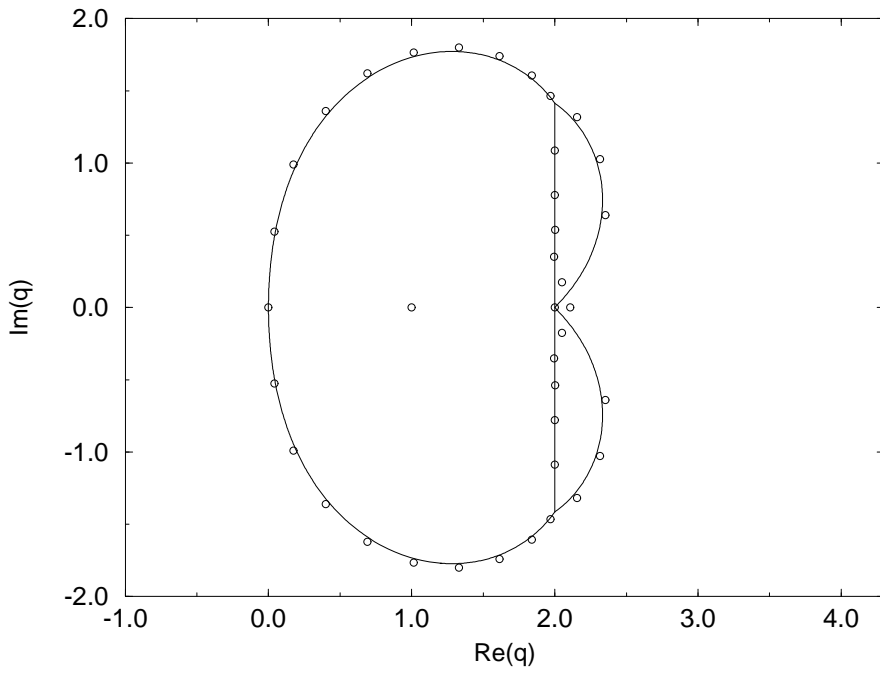


Figure 3: Diagram showing regional boundaries comprising \mathcal{B} for $W(\{L\}, q)$ for cyclic ladder graphs and zeros of $P(L_{2n}, q)$ for $2n = 38$.

$$|W(\{L\}, q)| = |1 - q| \quad \text{for } q \in R_2 \text{ or } R_2^* \quad (4.7.3)$$

$$|W(\{L\}, q)| = |3 - q| \quad \text{for } q \in R_3 \quad (4.7.4)$$

Formally, one can choose $1/n$ 'th roots so that $W(\{L\}, q) = 1 - q$ and $3 - q$ in the respective regions (R_2, R_2^*) and R_3 . Note that, in contrast to the situation with the bipyramid graphs B_n , there is no region where all $|a_j(q)| < 1$ so that the $c_0(q)$ term (which is equal to $q^2 - 3q + 1$ here) never dominates. The boundary between regions R_2 , R_2^* , and R_3 is the line $|1 - q| = |3 - q|$ where these are both leading terms, which is comprised of the line segments

$$\mathcal{B}(R_2, R_3) = \{q\} : \quad \text{Re}(q) = 2, \quad 0 < \text{Im}(q) < \sqrt{2} \quad (4.7.5)$$

and its complex conjugate for $\mathcal{B}(R_2^*, R_3)$. Similarly, the boundary separating R_1 from R_3 is the locus of solutions to the degeneracy condition $|q^2 - 3q + 3| = |3 - q|$ where these are leading terms. This boundary runs vertically through the origin $q = 0$ and extends over, on the right, to two complex-conjugate triple points $q = 2 \pm \sqrt{2}i$ where it meets the vertical line boundary (4.7.5) and its complex conjugate. Similarly, the boundaries separating R_1 from R_2 and R_1 from R_2^* are comprised of the locus of solutions to the degeneracy condition $|q^2 - 3q + 3| = |1 - q|$ where these are leading terms; as shown in Fig. 3, these boundaries extend from the above triple points over to a four-fold intersection point at $q = 2$. In passing, we note that our region diagram differs from that reported in Ref. [17], where the rightmost curves were thought to terminate and hence not completely separate from R_1 the two additional regions which we have identified as R_2 and R_2^* . In Fig. 3, we also show zeros of $P(L_{2n}, q)$ for $2n = 38$. We shall discuss these in Section 5.

4.8 Twisted Ladder (Möbius) Graphs

One may also consider ladder graphs the ends of which are twisted once before being joined; these graphs are denoted twisted ladder or Möbius graphs, M_{2n} . (It is easy to see that if one twists the ends an even number of times, this is equivalent to no twist, and any odd number of twists are equivalent to a single twist.) The chromatic polynomial is the same as that for L_{2n} except for the $c_0(q)$ term [17]

$$P(M_{2n}, q) = (q^2 - 3q + 3)^n + (q - 1)\{(3 - q)^n - (1 - q)^n\} - 1 \quad (4.8.1)$$

Since there is no region where the constant term $c_0(q)$ (equal to -1 here) is dominant, we find that

$$W(\{M\}, q) = W(\{L\}, q) \quad (4.8.2)$$

5 Theorem for Zeros of Chromatic Polynomials for Certain $\{G\}$

A general question which one may ask about zeros of chromatic polynomials is whether all, or some subset, of the zeros for an n -vertex graph G in the family $\{G\}$ lie exactly on the boundary curves \mathcal{B} . One knows that as $n \rightarrow \infty$, aside from the discrete general set of zeros of $P(G, q)$, viz., $q_0 = 0, 1$, and, for graphs containing one or more triangles, $q = 2$, the remainder of the zeros merge to form the union of boundaries \mathcal{B} separating various regions in the complex q plane. (Some of the set $\{q_0\}$ may also lie on \mathcal{B} .) However, the fact that the zeros move toward, and merge to form, this boundary \mathcal{B} in the $n \rightarrow \infty$ limit does not imply that, for finite graphs G , some subset of zeros will lie precisely on \mathcal{B} . We have investigated this question and have found that there do exist some families of graphs $\{G\}$ for which the zeros of $P(G, q)$ (aside from certain members of the set $\{q_0\}$) lie exactly on the respective boundary curves \mathcal{B} . We shall present a theorem and proof on this. Interestingly, we find that in all such cases, \mathcal{B} consists of a unit circle centered at a certain integral point on the positive real q axis. We emphasize, however, that this type of behavior is special and is not shared by other families of graphs that we have studied. Furthermore, for the families of graphs for which the theorem does hold, the positions of the unit circles differ for different $\{G\}$. Finally, as we shall show, the zeros populate the full circle with constant density.

We find that the theorem applies for the following three families of graphs: (i) cyclic; (ii) wheel, and (iii) biwheel. We begin with the cyclic graphs. The form of $P(C_n, q)$ differs depending on whether n is even, say $n = 2m$ or odd, say $n = 2m + 1$. For even $n \geq 4$, we calculate the factorization

$$P(C_{n=2m}, q) = q(q-1) \prod_{j=0}^{m-2} \left\{ q - \left(1 + e^{\frac{(2j+1)\pi i}{n-1}} \right) \right\} \left\{ q - \left(1 + e^{\frac{-(2j+1)\pi i}{n-1}} \right) \right\} \quad (5.1)$$

and for odd $n \geq 5$,

$$P(C_{n=2m+1}, q) = q(q-1)(q-2) \prod_{j=1}^{m-1} \left\{ q - \left(1 + e^{\frac{2j\pi i}{n-1}} \right) \right\} \left\{ q - \left(1 + e^{\frac{-2j\pi i}{n-1}} \right) \right\} \quad (5.2)$$

Special cases for lower n are $P(C_2, q) = q(q-1)$ and $P(C_3, q) = q(q-1)(q-2)$.

For the wheel graphs, for odd $n \geq 5$, we find the factorization

$$P((Wh)_{n=2m+1}, q) = q(q-1)(q-2) \prod_{j=0}^{m-2} \left\{ q - \left(2 + e^{\frac{(2j+1)\pi i}{n-2}} \right) \right\} \left\{ q - \left(2 + e^{\frac{-(2j+1)\pi i}{n-2}} \right) \right\} \quad (5.3)$$

and for even $n \geq 6$,

$$P((Wh)_{n=2m}, q) = q(q-1)(q-2)(q-3) \prod_{j=1}^{m-2} \left\{ q - \left(2 + e^{\frac{2j\pi i}{n-2}} \right) \right\} \left\{ q - \left(2 + e^{\frac{-2j\pi i}{n-2}} \right) \right\} \quad (5.4)$$

Special cases for lower n are $P((Wh)_3, q) = q(q-1)(q-2)$ and $P((Wh)_4, q) = q(q-1)(q-2)(q-3)$.

For the biwheel graphs we calculate for even $n \geq 6$,

$$P(U_{n=2m}, q) = q(q-1)(q-2)(q-3) \prod_{j=0}^{m-3} \left\{ q - \left(3 + e^{\frac{(2j+1)\pi i}{n-3}} \right) \right\} \left\{ q - \left(3 + e^{\frac{-(2j+1)\pi i}{n-3}} \right) \right\} \quad (5.5)$$

and for odd $n \geq 7$,

$$P(U_{n=2m+1}, q) = q(q-1)(q-2)(q-3)(q-4) \prod_{j=1}^{m-2} \left\{ q - \left(3 + e^{\frac{2j\pi i}{n-3}} \right) \right\} \left\{ q - \left(3 + e^{\frac{-2j\pi i}{n-3}} \right) \right\} \quad (5.6)$$

Special cases for lower n are $P(U_4, q) = q(q-1)(q-2)(q-3)$ and $P(U_5, q) = q(q-1)(q-2)(q-3)(q-4)$.

These factorizations constitute a proof of the following

Theorem 2

Except for isolated zeros at $q = 1$ for C_n , at $q = 0, 2$ for $(Wh)_n$, and at $q = 0, 1, 3$ for U_n , the zeros of $P(C_n, q)$, $P((Wh)_n, q)$, and $P(U_n, q)$ all lie on the respective unit circles $|q - q_\odot| = 1$ where $q_\odot(C_n) = 1$, $q_\odot(Wh_n) = 2$, and $q_\odot(U_n) = 3$. Furthermore, the zeros are equally spaced around the respective unit circles, and in the $n \rightarrow \infty$ limit, the density $g(\{G\}, \theta)$ of zeros on the respective circles $q = q_\odot + e^{i\theta}$, $-\pi < \theta \leq \pi$, is a constant, independent of θ . If one normalizes g according to

$$\int_{-\pi}^{\pi} g(\{G\}, \theta) d\theta = 1 \quad (5.7)$$

then

$$g(\{G\}, \theta) = \frac{1}{2\pi} \quad \text{for} \quad \{G\} = \{C\}, \{Wh\}, \{U\} \quad (5.8)$$

For the cyclic ladder and twisted ladder graphs L_{2n} and M_{2n} , we find the type of behavior which occurs with complex-temperature zeros of spin models: the zeros lie close to, but not, in general, precisely on, the asymptotic boundaries \mathcal{B} . This is illustrated by the plots of zeros of $P(L_{38}, q)$ in Fig. 3. As one also finds in calculations of complex-temperature zeros in statistical mechanical spin models (see, e.g., [21, 22]), the densities of zeros along certain boundary curves are very small; in Fig. 3 this occurs on $\mathcal{B}(R_1, R_2)$ near the intersection point $q = 2$. Similar low densities of zeros were observed for $P(tri, q)$ on the boundary near $q = 0$ and the right-most boundary near $q = 4$ [14]. In statistical mechanics, the density of zeros g near a critical point z_c behaves as

$$g \sim |z - z_c|^{1-\alpha'} \quad (5.9)$$

where α' denotes the critical exponent describing the (leading) singularity in the specific heat at $z = z_c$ as one approaches this point from within the broken-symmetry phase: $C_{sing} \sim |z - z_c|^{-\alpha'}$ [21]. Equivalently, the (leading) singularity in the free energy at $z = z_c$ is given by $f_{sing} \sim |z - z_c|^{2-\alpha'}$. (Similar statements apply for the approach to z_c from within the symmetric phase with the replacement $\alpha' \rightarrow \alpha$.) Analogously, in the present context, the density of zeros of $P(G, q)$ for a finite- n graph G near a singular point is determined by the nature of the singularity in the asymptotic function $W(\{G\}, q)$: if one denotes the singularity in the function $\ln W(\{G\}, q)$ at a point q_c as

$$\ln W(\{G\}, q)_{sing} \sim |q - q_c|^{2-\alpha'_\phi} \quad (5.10)$$

where α'_ϕ will, in general, depend on the direction (ϕ) of approach to q_c , then the corresponding density of zeros of $P(\{G\}, q)$ as one approaches this point is

$$g(\{G\}, q) \sim |q - q_c|^{1-\alpha'_\phi} \quad (5.11)$$

For the bipyramid, as is evident in Fig. 2, we find that, except for the general zeros at $q = 0$ and 1 and a zero very near to $q = Be_5 = 2.618\dots$, the inner zeros do lie near to the arcs forming the boundaries $\mathcal{B}(R_1, R_3)$ and $\mathcal{B}(R_2, R_3)$, but the outer zeros do not lie very close to the line segments of $\mathcal{B}(R_1, R_2)$, given by eq. (4.6.7), and only approach these line segments slowly as n increases. Since this latter behavior only occurs for the part of \mathcal{B} extending to $q = 5/2 \pm i\infty$, it is plausible that it may be connected with the fact that this component of the boundary is noncompact. This inference is also consistent with the fact that of the families of graphs which we have studied, the bipyramid graphs form the only family with a noncompact \mathcal{B} and the only family for which we have observed this deviation.

6 Theorem on Singular Boundary of $W(\Lambda, q)$

In recent work [22]-[24] on complex-temperature and Yang-Lee (complex-field) singularities of Ising models, it has been quite fruitful to carry out a full complexification of both the temperature-dependent Boltzmann weight $u = z^2 = e^{-4K}$ and the field-dependent Boltzmann weight $\mu = e^{-2\beta H}$ and to study the singularities in the two-dimensional C^2 manifold depending on (z, μ) or (u, μ) . This approach unifies the previously separate analyses of complex-temperature and Yang-Lee singularities; one sees that a given singular point (z_c, μ_c) or (u_c, μ_c) in the C^2 manifold manifests itself as a singular point in the complex z or u plane for a fixed μ and equivalently as a singular point in the complex μ plane for fixed z or u .

We find this approach to be equally powerful here. Starting from the relation (1.6) between the chromatic polynomial and the $T = 0$ Potts antiferromagnet on a graph G , we

consider the two-dimensional complex manifold C^2 spanned by (a, q) (where a was defined in eq. (1.5)). For sufficiently large q , namely, $q > 2\zeta$, where ζ is the coordination number of the lattice $G = \Lambda$, the Dobrushin theorem implies [25] that the Potts antiferromagnet is disordered, with exponential decay of correlation functions, at $T = 0$. As one decreases q , the AFM ordering tendency of the system increases, and, as q decreases through a critical value depending on the dimensionality d and lattice Λ , the model can become critical at $T = 0$, or equivalently, $K = -\infty$. As one decreases q further, the AFM critical temperature increases from zero to positive values (i.e. K_c increases from $-\infty$ to a finite negative value). The critical value q_c thus separates two regions in q : (i) the $q > q_c$ region, where the system is disordered at $T = 0$ and (ii) an interval of $q < q_c$ where the system has AFM long-range order at $T = 0$ (and for a finite interval $0 \leq T \leq T_c$, where $K_c = J/(k_B T_c)$). Now, using the relations (1.6), (1.7) and making the projection from the (a, q) space onto the real a axis, just as the disordered, Z_N -symmetric phase of the Potts AF must be separated by a non-analytic phase boundary from the broken-symmetry phase with AFM long-range order [26], so also, making the projection onto the real q axis for the $W(\Lambda, q)$ function, it follows that the range $q > q_c$ and an adjacent interval $q < q_c$ must be separated by a non-analytic boundary. Furthermore, just as, by analytic continuation, the complex-temperature extension of the disordered phase of the Potts antiferromagnet must be completely separated by a non-analytic phase boundary from the complex-temperature extension of the antiferromagnetically ordered phase, so also the region in the complex q plane containing the line segment $q > q_c$ must be completely separated from the region containing the adjacent interval to the left of q_c in this plane. Since the zero-temperature criticality of the Potts AF and the critical value q_c are both projections of the singular point $(a_c = 0, q_c)$ in the C^2 manifold, we have derived the following theorem:

Theorem 3: For a given lattice Λ , the point q_c at which the right-most region boundary for $W(\Lambda, q)$ crosses the real q axis corresponds to the value of q at which the critical point a_c of the Potts antiferromagnet on this lattice first passes through zero as one decreases q from large positive values.

This point q_c is the maximal finite real point of non-analyticity of $W(\Lambda, q)$.

We now discuss the application of this theorem to three specific 2D lattices. For this purpose, we recall that the q -state Potts model can be defined for non-integral as well as integral values of q because of the equivalent representation of the partition function [7]-[9], [27]

$$Z = \sum_{G' \subseteq G} v^{b(G')} q^{n(G')} \quad (6.1)$$

where G' denotes a subgraph of $G = \Lambda$, $v = (a - 1)$, $b(G')$ is the number of bonds and $n(G')$ the number of connected components of G' . (Recall that one can see the connection of this with (1.6) by taking the $K \rightarrow -\infty$ ($v \rightarrow -1$) limit of (6.1), which yields the Whitney expression for $P(G, q)$ [2].)

6.1 q_c for the Honeycomb Lattice

For the honeycomb (hc) lattice, the paramagnetic-ferromagnetic (PM-FM) and PM-AFM critical points are both determined by the equation [28]

$$q^2 + 3q(a - 1) - (a - 1)^3 = 0 \quad (6.1.1)$$

As q decreases in the range from 4 to $q = Be_5 = 2.618$, one of the roots of eq. (6.1.1) increases from -1 to 0. This root can be identified as the AFM critical point $a_c(q)$ by going in the opposite direction, increasing q from its Ising value, $q = 2$ and tracking $a_c(q)$, which decreases from $a_c(2) = 2 - \sqrt{3}$ to $a(q = Be_5) = 0$, where the AFM phase is squeezed out and there is no longer any finite-temperature AFM critical point, which now occurs only at $T = 0$. Hence, our theorem implies that

$$q_c(hc) = \frac{3 + \sqrt{5}}{2} = Be_5 = 2.618.. \quad (6.1.2)$$

i.e., this is the value of q where the right-most regional boundary of $W(hc, q)$ crosses the real axis in the complex q plane [36]. We may compare this with the numerical calculation of zeros of $P(hc, q)$, as a function of q , on finite honeycomb lattices in Ref. [14]. For this comparison, we first note that from the analogous study of the triangular lattice [14], one sees the crossing point of a boundary curve increases by about $\Delta q \simeq 0.4$ from an 8×8 triangular lattice with cylindrical boundary conditions (CBC's) to the thermodynamic limit. Assuming that a similar finite-size shift occurs for the honeycomb lattice, and noting that the curve of zeros calculated on the 8×8 hc lattice with CBC's cross the real axis at $q \simeq 2.2$, we find that these numerical results are consistent with the result of Theorem 3 for the thermodynamic limit.

6.2 q_c for the Square Lattice

For the square lattice, the PM-AFM critical point of the Potts antiferromagnet is given by [29]

$$(a + 1)^2 = 4 - q \quad (6.2.1)$$

i.e.,

$$a_c(sq) = -1 + \sqrt{4 - q} \quad (6.2.2)$$

As q decreases from 4 to 3, this value of a_c increases from -1 to 0. Hence,

$$q_c(sq) = 3 \quad (6.2.3)$$

Our Theorem 3 then identifies $q_c(sq)$ as the point where the right-most region boundary of $W(sq, q)$ crosses the real axis in the complex q plane. Using the same rough estimate for the finite-size shift between the 8×8 square lattice with CBC's and the thermodynamic limit as was observed for the triangular lattice, viz., $\Delta q \simeq 0.4$ and noting that a curve of zeros calculated for this finite square lattice crosses the real axis at $q \simeq 2.6$ [14], we see that our inference (6.2.3) is consistent with the numerical calculations in Ref. [14].

6.3 q_c for the Triangular Lattice

Baxter's exact solution for $W(tri, q)$ [14] shows that in this case,

$$q_c(tri) = 4 \quad (6.3.1)$$

where the right-most boundary, $\mathcal{B}(R_1, R_2)$, crosses the real q axis. Theorem 3 implies that the two other singular points where the boundaries $\mathcal{B}(R_2, R_3)$ and $\mathcal{B}(R_3, R_1)$ cross this axis, at $q = 3.82\dots$ and $q = 0$, respectively, also correspond to singular points of the Potts antiferromagnet in the a plane at these two q values.

7 Numerical Calculations of $W(\Lambda, q)$ for $\Lambda = sq, hc, tri$

The effect of ground state disorder and associated nonzero ground state entropy S_0 has been a subject of longstanding interest. A physical example is ice, for which $S_0 = 0.82 \pm 0.05$ cal/(K-mole), i.e., $S_0/k_B = 0.41 \pm 0.03$ [30, 31]. In statistical mechanical models, such a ground state entropy may occur in contexts such as the Ising (or equivalently, $q = 2$ Potts) antiferromagnet on the triangular [32] or kagomé [33] lattices, where there is frustration. However, ground state entropy can also occur in what is arguably a simpler context: one in which it is not accompanied by any frustration. On a given lattice, for sufficiently large q , Potts antiferromagnets exhibit ground state entropy without frustration; restricting to integral values of q , this is true for $q \geq 3$ on the square and honeycomb lattices, and for $q \geq 4$ on the triangular lattice [34]. For the given range of q on the respective lattices, since the internal energy U approaches its $T = 0$ value $U(T = 0) = -J\langle\delta_{\sigma_i\sigma_j}\rangle_{T=0} = 0$ exponentially fast, it follows that for $T \rightarrow 0$, i.e., $K \rightarrow -\infty$, $\lim_{K \rightarrow -\infty} \beta U = 0$. Hence, from

the general relation $S = \beta U + f$, it follows that, for this range of values of q , the ground state entropy (per site) and reduced free energy for the Potts antiferromagnet are related according to

$$S_0(\Lambda, q) = f(\Lambda, q, K = -\infty) = \ln W(\Lambda, q) \quad (7.1)$$

and hence $W(\Lambda, q)$ is a measure of this ground state entropy. Accordingly, it is of interest to calculate $W(\Lambda, q)$ for various lattices Λ and values of q . Moreover, from a mathematical point of view, for positive integer q , the numerical calculation of $W(\Lambda, q)$ gives an accurate measure of the asymptotic growth of $P(\Lambda, q) \sim W(\Lambda, q)^n$ as the number of lattice sites $n \rightarrow \infty$.

Extending our earlier calculation of $W(hc, 3)$ [36], we have calculated $W(hc, q)$ for integer $4 \leq q \leq 10$. We use the relation for the entropy

$$S(\beta) = S(\beta = 0) + \beta U(\beta) - \int_0^\beta U(\beta') d\beta' \quad (7.2)$$

which is known to provide a very accurate method for calculating S_0 [35]. We start the integration at $\beta = 0$ with $S(\beta = 0) = \ln q$ for the q -state Potts antiferromagnet and utilize a Metropolis algorithm with periodic BC's for several $L \times L$ lattices with the length L varying over the values 4,6,8,10,12,14, and 16 for all cases, and up to $L = 24$ for certain cases. Since $U(K)$ very rapidly approaches its asymptotic value of 0 as K decreases past about $K = -5$, the RHS of (7.2) rapidly approaches a constant in this region, enabling one to obtain the resultant value of $S(\beta = \infty)$ for each lattice size. For each value of q , we then perform a least squares fit to this data and extrapolate the result to the thermodynamic limit, and then obtain W from (7.1). We use double precision arithmetic for all of our computations. Typically, we ran several thousands sweeps through the lattice for thermalization before calculating averages. Each average was calculated using between 9,000 and 20,000 sweeps through the lattice. As we have discussed in Ref. [36], for $q \geq 3$ on the honeycomb lattice (and also for $q \geq 4$ on square lattice), the finite-size dependence of S_0 is not simply of the form $S_0(\Lambda; L \times L, q) = S_0(\Lambda, q) + c_{\Lambda,1}^{(q)} L^{-2}$; we fit our measurements with an empirical function of the form

$$S_0(\Lambda; L \times L, q) = S_0(\Lambda, q) + c_{\Lambda,1}^{(q)} L^{-2} + c_{\Lambda,2}^{(q)} L^{-4} + c_{\Lambda,3}^{(q)} L^{-6} \quad (7.3)$$

As an example, we show in Fig. 4 the ground state entropy as a function of L^{-2} , for the case $q = 4$ on the square and honeycomb lattices. As a check, we have confirmed that our measurements yield numbers consistent with the exact result $S_0 = 0$ for $q = 2$ and $\Lambda = hc, sq$.

In the course of these calculations, we have obtained a measurement of $W(hc, 3)$ which is more accurate than, and in excellent agreement with, the value that we reported recently in Ref. [36] (where we quoted the uncertainty conservatively). This improvement is due to our

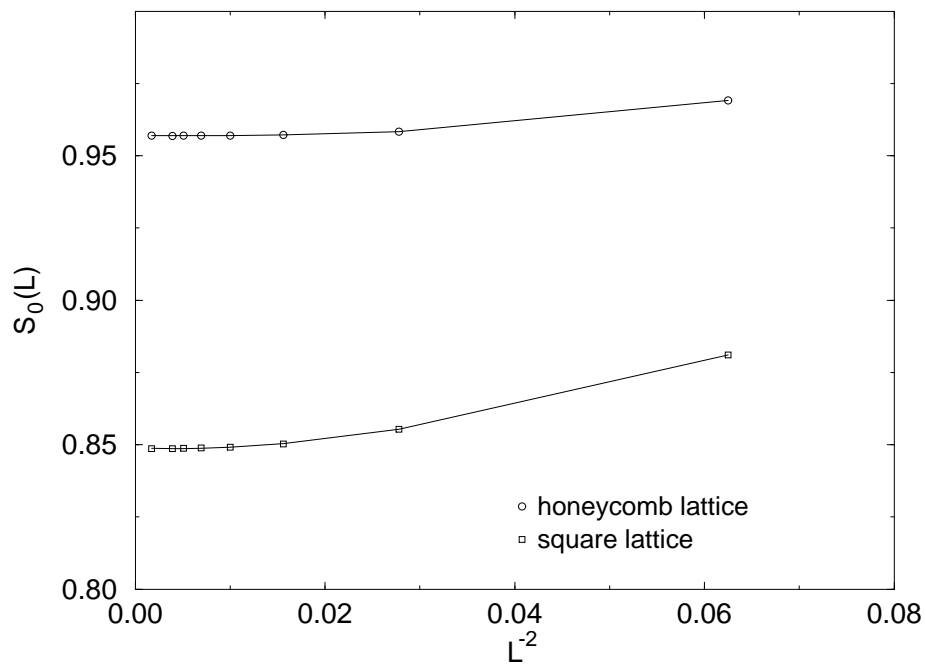


Figure 4: Measurements of ground state entropy S_0 , as a function of lattice size, for the $q = 4$ Potts AF on the honeycomb and square lattices.

q	$W(hc, q)$	hc series	$W(sq, q)$	sq series
3	1.6600(10)	1.6874	1.53965(90)	1.5396007..
4	2.6038(15)	2.6088	2.3370(15)	2.3361
5	3.5796(20)	3.5812	3.2510(20)	3.2504
6	4.5654(30)	4.5658	4.2003(25)	4.2001
7	5.5556(35)	5.5556	5.1669(30)	5.1667
8	6.5479(40)	6.5483	6.1431(40)	6.1429
9	7.5424(45)	7.5427	7.1254(45)	7.1250
10	8.5386(50)	8.5383	8.1122(50)	8.1111

Table 1: Values of $W(\Lambda, q)$ for $\Lambda = hc, sq$ and $3 \leq q \leq 10$ from Monte Carlo measurements, compared with large- q series. The entry for $W(sq, 3)$ is from the exact expression. See text for further details.

use of larger lattices, up to 24×24 , and double precision arithmetic, in the present work. Our results for $W(hc, q)$ are presented in Table 1 (with conservatively estimated uncertainties given in parentheses) and plotted in Fig. 5, together with the respective values obtained by evaluating the large- q series of Ref. [20]. For a lattice Λ , this series has the form

$$W(\Lambda, q) = q \left(\frac{q-1}{q} \right)^{\zeta/2} \overline{W}(\Lambda, q) \quad (7.4)$$

where, as above, ζ is the lattice coordination number, and

$$\overline{W}(\Lambda, q) = 1 + \sum_{n=1}^{\infty} w_n y^n, \quad y = \frac{1}{q-1} \quad (7.5)$$

For the honeycomb lattice, $\overline{W}(hc, q) = 1 + y^5 + 2y^{11} + 4y^{12} + \dots$, calculated through $O(y^{18})$ [20]. Because of the sign changes in the hc series (the coefficients of the first five terms are positive, while those of the remaining four terms are negative), it is difficult to make a reliable extrapolation. Accordingly, for Table 1 and Fig. 5 we simply use a direct evaluation of the sum. As is evident from this figure, the agreement with our Monte Carlo calculation is excellent. From our result (6.1.2) above (see also our Ref. [36]), it follows that the large- q series cannot be applied below $q = 2.62$, and we have plotted it only down to the integer value, $q = 3$. For both the honeycomb and square lattices, we also show the exact results $W(\Lambda, 2)_{D_{nq}} = 1$ for $\Lambda = hc, sq$ (as a superimposed circle and square) and $W(\Lambda, 0)_{D_{nq}} = W(\Lambda, 1)_{D_{nq}} = 0$ (as a dot \bullet), but we emphasize that these values assume the order of the limits in the definition D_{nq} in eq. (2.14) and the respective values calculated with the other

order of limits in the definition D_{qn} in eq. (2.13) for these lattices (which values are not known exactly) could well be different from these D_{nq} values.

It is also of interest to compare $W(\Lambda, q)$ for the other two regular 2D lattices, square and triangular. Unlike the honeycomb lattice, there have been previous Monte Carlo measurements for the square lattice [41] for lattice sizes between 3×3 and 7×7 and q values up to 10. We have extended these to considerably larger lattices, including 16×16 for all q values. As a check, for $q = 3$, from calculations on $L \times L$ lattices with periodic boundary conditions, for $L = 4, 6, 8, 10, 12, 14$ and 16 , we obtain the fit

$$S_0(sq, 3) = 0.431556 + 1.095289L^{-2} \quad (7.6)$$

This yields an asymptotic value which is in excellent agreement with the exact result [37] $S_0(sq, 3) = (3/2) \ln(4/3) = 0.43152311\dots$ (i.e., $W(sq, 3) = 1.5396007\dots$);

$$\frac{|S_0(sq, 3)_{exact} - S_0(sq, 3)_{MC}|}{S_0(sq, 3)_{exact}} = 0.76 \times 10^{-4} \quad (7.7)$$

The coefficient of the L^{-2} term agrees with a previous determination for this $q = 3$ case [38]. Our fitting procedure for $q \geq 4$ has been discussed in conjunction with eq. (7.3) above. We also compare our Monte Carlo calculations with the large- q series, (7.4), (7.5) which, for $\Lambda = sq$ was calculated to $O(y^{18})$ in Ref. [20]. The agreement is again excellent. In passing, we note that a calculation of the series for $\overline{W}(sq, q)$ to order $O(y^{36})$ has been reported in Ref. [42], but we have checked that additional terms in this longer series have a negligible effect in the comparison of the series with our numerical results. Given our result that $q_c(sq) = 3$ in (6.2.3), the large- q series cannot be applied for $q < 3$. It is interesting that the agreement between the series and our measurements is quite good even down to the respective region boundaries which we have deduced at $q_c(hc) = 2.618$ and $q_c(sq) = 3$. This suggests that the non-analyticities at these respective points on the honeycomb and square lattices are evidently not so strong as to cause the series to deviate strongly from the actual values of $W(\Lambda, q)$.

In passing, we remark that of course our results are consistent with the following rigorous bounds: (i) the general upper bound $W(\Lambda, q) < q$; (ii) the upper bound for the square lattice [39], $W(sq, q) \leq (1/2)(q - 2 + \sqrt{q^2 - 4q + 8})$, which is more restrictive than (i) for $q > 1/2$; (iii) the lower bound applicable for any bipartite lattice, $W(\Lambda_{bip.}, q) \geq \sqrt{q - 1}$; and (iv) the lower bound for the square lattice [39], $W(sq, q) \geq (q^2 - 3q + 3)/(q - 1)$. Note that for $q = 2$, both lower bounds (iii) and (iv) are realized as equalities, $W(sq, 2) = 1$. Although there is a range of q above 2 where (iv) lies below (iii), for $q \geq 3$, (iv) lies above (iii), i.e. is more restrictive. Some recent rigorous upper bounds on $P(G, q)$ for general G have been given in

Ref. [40], but these only improve the prefactor A multiplying $P(G, q) \leq Aq^n$, and hence still yield $W(G, q) \leq q$, as in (i).

In the case of the triangular lattice, since, to our knowledge, there is no numerical evaluation in the literature of the expressions for $W(tri, q)$ given in Ref. [14], we have carried this out and plotted the resultant function in Fig. 5. The point $q = 3$ is an example of a special point q_s discussed in section 2, where the behavior of $P(G, q)$ changes abruptly from (2.9) to (2.10) and where, consequently, the two limits in (1.9) do not commute. As noted above, since there are just 6 ways of coloring a triangular lattice (equivalently, the ground state of the Potts AF is 6-fold degenerate), $W(tri, 3)_{D_{nq}} = 1$. We have indicated this with a symbol Δ in Fig. 5. However, with the other order of limits, (2.13), $\lim_{q \rightarrow 3} W(tri, q) = W(tri, 3)_{D_{qn}} \neq 1$. (The actual value is $W(tri, 3)_{D_{qn}} = 2$.) In Fig. 5, at the other special points $q_s = 0, 1$ (indicated with \bullet) and $q_s = 2$ (indicated with Δ) we have shown the values $W(tri, q)_{D_{nq}} = 0$. Again, however, because of the noncommutativity of limits in (1.9) as discussed in section 2, the value of $W(tri, q)_{D_{qn}}$ calculated with the other order of limits, (2.13) is nonzero. At $q = 1, 2$, it is positive, while at $q = 0$, the function has a discontinuity involving a flip in sign:

$$\lim_{q \rightarrow 0^-} W(tri, q) = - \lim_{q \rightarrow 0^+} W(tri, q) \quad (7.8)$$

The sign of $W(tri, q)$ for negative real q is unambiguous, since this interval is part of the region R_1 and where consequently, there is a clear choice of $1/n$ 'th root, given by $r = 0$, in (1.3). This is also clear from the large- q series [20]. In Refs. [13, 14], it was noted that the transfer matrix calculation used there can fail at the Beraha numbers $q = Be_r$; from the discussion that we have given in section 2 of this paper, we would view this as a specific realization of the general noncommutativity of limits (1.9).

A general property one observes in Fig. 5 is that for these three lattices, for a fixed value of q in the range $q \geq 4$, $W(\Lambda, q)$ is a monotonically decreasing function of the lattice coordination number ζ and a monotonically increasing function of the lattice ‘‘girth’’ γ , defined [5] as the number of bonds, or equivalently, vertices contained in a minimum-distance circuit. Here, $\zeta = 3, 4, 6$ and $\gamma = 6, 4, 3$ for $\Lambda = hc, sq, tri$. The dependence on the girth is easily understood: the smaller the girth, the more stringent is the constraint that no two colors on adjacent vertices can be the same. Concerning the dependence on ζ , we note that for tree graphs, where one can vary ζ for fixed γ ($\gamma = \infty$), $P(T_n, q)$ and hence $W(\{T\}, q)$ are actually independent of ζ (c.f. eq. (4.1.1)). This is also true for the magnitude $|W(\Lambda, q)|$ for real negative q .

For the bipartite (square and honeycomb) lattices, we observe the following general trend:

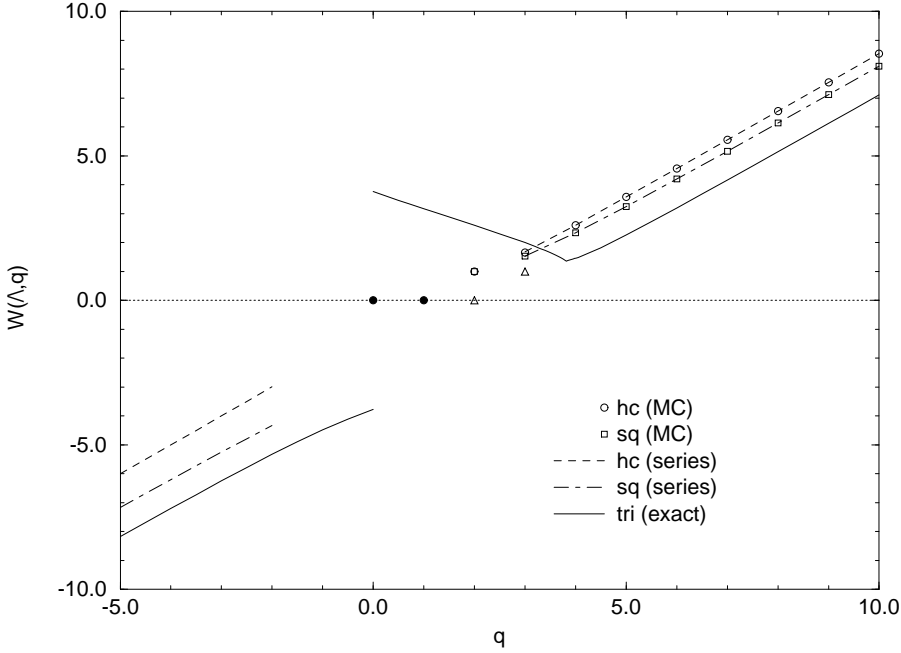


Figure 5: Plot of $W(\Lambda, q)$ for $\Lambda = sq, hc, tri$. At the special points $q_s = 0, 1$ for all lattices, the zero values (denoted by the symbol \bullet) apply for the order of limits in the definition D_{nq} in eq. (2.14). For the triangular lattice at the special points $q_s = 2, 3$, the respective values 0 and 1 (denoted by the symbol Δ) also apply for this ordering of limits (2.14), as does the value $W(\Lambda, 2)_{D_{nq}} = 1$ for $\Lambda = sq, hc$. The $\Lambda = tri$ curve is plotted for the definition D_{qn} in eq. (2.13).

as q increases from $q = 3$, the ratios

$$r_W(\Lambda, q) = \frac{W(\Lambda, q)}{W(\Lambda, q)_{max}} = \frac{W(\Lambda, q)}{q} \quad (7.9)$$

and the related

$$r_S(\Lambda, q) = \frac{S(\Lambda, q; T = 0)}{S(\Lambda, q, T = \infty)} = \frac{\ln(W(\Lambda, q))}{\ln q} \quad (7.10)$$

are monotonically increasing functions of q . The ratio $r_S(\Lambda, q)$ has a physical interpretation as measuring the residual disorder present in the q -state Potts antiferromagnet at $T = 0$, relative to its value at $T = \infty$. This ratio is substantial; for example, from Table 1, one sees that $r_S(hc, 3) = 0.461$ and $r_S(sq, 3) = (3/2) \ln(4/3) / \ln 3 = 0.393$ while $r_S(hc, 10) = 0.931$ and $r_S(sq, 10) = 0.909$. On the triangular lattice, as q increases from $q = 4$, one again finds that r_W and r_S monotonically increase; for example, $r_S(tri, 4) = 0.273$ while $r_S(tri, 10) = 0.852$.

Returning to the square and honeycomb lattices, although we cannot use our Monte Carlo method to evaluate $W(hc, q)$ for negative q , we can use the large- q series, since the negative q axis is in the region R_1 . Of course these series cannot be used all the way in to $q = 0$; in Fig. 5, we plot them up to $q = -2$.

8 Conclusions

In conclusion, we have presented some results on the analytic properties of the asymptotic limiting function $W(\{G\}, q)$ obtained from the chromatic polynomial $P(G, q)$. We have pointed out that the formal equation (1.1) is not, in general, sufficient to define the function $W(\{G\}, q)$ because of the noncommutativity of limits (1.9) at certain special points, and we have provided the necessary clarification for a complete definition of this asymptotic function. Using mathematical results on chromatic polynomials for several families of graphs $\{G\}$, we have calculated $W(\{G\}, q)$ exactly for these families. From these results, we have determined the non-analytic boundaries separating various regions in the complex q plane for each of the $W(\{G\}, q)$. We have also studied the zeros of chromatic polynomials for these families of graphs and have proved a theorem stating that for some families, all but a finite set of these zeros lie exactly on certain unit circles centered at positive integer points on the real q axis. Using the connection of chromatic polynomials to the partition function of the q -state Potts antiferromagnet on a lattice Λ at $T = 0$, in conjunction with a generalization to both complex q and complex temperature, we have presented another theorem specifying the position of the maximal (finite) real point $q_c(\Lambda)$ where $W(\{G\} = \Lambda, q)$ is non-analytic and have applied this to determine q_c on the square and honeycomb lattices. Finally, we have given Monte

Carlo measurements of $W(hc, q)$ (and $W(sq, q)$) for integral $3 \leq q \leq 10$ and compared these with large- q series. Our results illustrate the fascinating and deep connections between the mathematics of chromatic polynomials and their limits on the one hand, and the statistical mechanics of antiferromagnetic Potts models on the other.

This research was supported in part by the NSF grant PHY-93-09888.

References

- [1] G. D. Birkhoff, *Ann. of Math.* **14**, 42 (1912).
- [2] H. Whitney, *Ann. of Math.* **33**, 688 (1932); *Bull. Am. Math. Soc.* **38**, 572 (1932).
- [3] G. D. Birkhoff and D. C. Lewis, *Trans. Am. Math. Soc.* **60**, 355 (1946).
- [4] R. C. Read and W. T. Tutte, "Chromatic Polynomials", in *Selected Topics in Graph Theory, 3*, eds. L. W. Beineke and R. J. Wilson (Academic Press, New York, 1988).
- [5] W. T. Tutte *Graph Theory*, vol. 21 of *Encyclopedia of Mathematics and its Applications*, ed. Rota, G. C. (Addison-Wesley, New York, 1984).
- [6] R. B. Potts, *Proc. Camb. Phil. Soc.* **48**, 106 (1952).
- [7] P. W. Kasteleyn and C. M. Fortuin, *J. Phys. Soc. Jpn. Suppl.* **26**, 11 (1969); C. M. Fortuin and P. W. Kasteleyn, *Physica* **57**, 536 (1972).
- [8] F. Y. Wu, *Rev. Mod. Phys.* **54**, 235 (1982).
- [9] R. J. Baxter, *Exactly Solved Models in Statistical Mechanics* (Academic Press, New York, 1982).
- [10] As is well-known, boundary conditions do not affect the thermodynamic limit except in the sense that they can affect which of degenerate ground states the system picks in the broken-symmetry phase.
- [11] R. J. Baxter, *J. Math. Phys.* **11**, 784 (1970).
- [12] N. L. Biggs, *J. Phys. A* **8**, L110 (1975).
- [13] R. J. Baxter, *J. Phys. A* **19**, 2821 (1986).
- [14] R. J. Baxter, *J. Phys. A* **20**, 5241 (1987).

- [15] V. Matveev and R. Shrock, *J. Phys. A* **28**, 5235 (1995).
- [16] F.-M. Dong and Y. Liu, *Discrete Math.* **145**, 95 (1995).
- [17] N. L. Biggs, R. M. Damerell, and D. A. Sands, *J. Combin. Theory B* **12**, 123 (1972).
- [18] S. Beraha and J. Kahane, *J. Combin. Theory B* **27**, 1 (1979); S. Beraha, J. Kahane, and N. Weiss, *ibid.*, **28**, 52 (1980).
- [19] C. N. Yang and T. D. Lee, *Phys. Rev.* **87**, 404 (1952); T. D. Lee and C. N. Yang, *ibid.* **87**, 410 (1952).
- [20] D. Kim and I. G. Enting, *J. Combin. Theory, B* **26**, 327 (1979).
- [21] R. Abe, *Prog. Theor. Phys.* **38**, 322 (1967).
- [22] V. Matveev and R. Shrock, *J. Phys. A* **28**, 4859 (1995).
- [23] V. Matveev and R. Shrock, *Phys. Rev.* **E53**, 254 (1996).
- [24] V. Matveev and R. Shrock, *Phys. Lett.* **A215**, 271 (1996).
- [25] R. L. Dobrushin, *Theor. Prob. and Applic.* **13**, 197 (1968)); *Theor. Prob. and Applic.* **15**, 458 (1970); J. Salas and A. Sokal, cond-mat/9603068.
- [26] This boundary itself has a complex-temperature extension which can be probed via calculations of zeros of the Potts partition function; see C. N. Chen, C. K. Hu, and F. Y. Wu, *Phys. Rev. Lett.* **76**, 169 (1996); F. Y. Wu et al., *ibid.* **76**, 173 (1996); V. Matveev and R. Shrock, *Phys. Rev.* **E54**, 6174 (1996); and, for earlier work, P. P. Martin, *Potts Models and Related Problems in Statistical Mechanics* (World Scientific, Singapore, 1991).
- [27] R. J. Baxter, *J. Phys. C* **6**, L445 (1973).
- [28] D. Kim and R. Joseph, *J. Phys. C* **7**, L167 (1974); R. J. Baxter, H. N. V. Temperley, and S. Ashley, *Proc. Roy. Soc. London, Ser. A* **358**, 535 (1978); T. W. Burkhardt and B. W. Southern, *J. Phys. A* **11**, L247 (1978).
- [29] R. J. Baxter, *Proc. Roy. Soc. London, Ser. A* **383**, 43 (1982).
- [30] W. F. GIAUQUE and J. W. STOUT, *J. Am. Chem. Soc.* **58**, 1144; (1936); L. Pauling *The Nature of the Chemical Bond* (Cornell Univ. Press, Ithaca, 1936; 3rd. ed. 1960), p. 466.

- [31] E. H. Lieb and F. Y. Wu, in C. Domb and M. S. Green, eds., *Phase Transitions and Critical Phenomena* (Academic Press, New York, 1972) v. 1, p. 331.
- [32] G. H. Wannier, Phys. Rev. **79**, 357 (1950).
- [33] K. Kano and S. Naya, Prog. Theor. Phys. **10**, 158 (1953); S. Suto, Z. Phys. B **44**, 121 (1981).
- [34] Ground state entropy without frustration can also occur in models with continuous variables and interactions; an example is studied in G. Kohring and R. Shrock, Nucl. Phys. B **295**, 36 (1988).
- [35] K. Binder, Zeit. f. Physik **B45**, 61 (1981).
- [36] R. Shrock and S.-H. Tsai, cond-mat/9608095, J. Phys. A, in press.
- [37] E. H. Lieb, Phys. Rev. **162**, 162 (1967).
- [38] J.-S. Wang, R. H. Swendsen, and R. Kotecký, Phys. Rev. B **42**, 2465 (1990).
- [39] N. L. Biggs, Bull. London Math. Soc. **9**, 54 (1977). We note that the lower bound for $W(sq, q)$ from this work coincides with the $d = 2$ special case of an estimated lower bound applicable to d -dimensional cartesian lattices Λ_d , viz., $W(\Lambda_d, q) \geq 1 + (q - 2)^d / (q - 1)^{d-1}$, presented in D. C. Mattis, Int. J. Mod. Phys. **B1**, 103 (1987). See also Y. Chow and F. Y. Wu, Phys. Rev. **B36**, 285 (1987).
- [40] F. Lazebnik, J. Graph Theory **14**, 25 (1990); K. Dohmen, J. Graph Theory **17**, 75 (1993).
- [41] X. Chen and C. Y. Pan, Int. J. Mod. Phys. **B1**, 111 (1987); C. Y. Pan and X. Chen, *ibid.* **B2**, 1503 (1988).
- [42] A. V. Bakaev and V. I. Kabanovich, J. Phys. A **27**, 6731 (1994).
- [43] V. Matveev and R. Shrock, J. Phys. A **29**, 803 (1996).